Visualization of pentatopic meshes

Guillem Belda-Ferrín*, Eloi Ruiz-Gironés*, Xevi Roca *
*Barcelona Supercomputing Center, Barcelona, Spain
E-mail: {guillem.belda, eloi.ruizgirones, xevi.roca}@bsc.es

***Abstract*—We propose a simple tool to visualize 4D unstructured pentatopic meshes. The method slices unstructured 4D pentatopic meshes (fields) with an arbitrary 3D hyperplane and obtains a conformal 3D unstructured tetrahedral representation of the mesh (field) slice ready to explore with standard 3D visualization tools. The results show that the method is suitable to visually explore 4D unstructured meshes. This capability has facilitated devising our 4D bisection method, and thus, we think it might be useful when devising new 4D meshing methods. Furthermore, it allows visualizing 4D scalar fields, which is a crucial feature for our space-time applications.**

Keywords*—*Visualization, 4D mesh, pentatopic mesh

I. Extended Abstract

In the last years, there has been an emerging interest to generate [1], [2], refine [3], [4], [5], [6], [7], [8], and adapt [9] 4D meshes. In our case, the need to simulate unsteady problems using full space-time (3D space + 1D time) discretizations with unstructured methods prompts our interest. We think that one key issue that is hampering to devise, check, and illustrate new 4D meshing approaches is the lack of a natural approach to visualize 4D meshes. We aim to provide a preliminary solution to this issue, by providing a simple tool to visualize 4D unstructured pentatopic meshes.

Our method is devised to exploit existent 3D visualization software which provides mature user interfaces to interact in real-time with 2D projections of the 3D meshes. To exploit these interfaces, we propose to slice unstructured 4D pentatopic meshes (fields) with an arbitrary 3D hyperplane and obtain a conformal 3D unstructured tetrahedral representation of the mesh (field) slice that is ready to be read with standard 3D visualization tools. Recently, a method to visualize 4D pentatopic meshes has been outlined in [9]. The main difference with our approach is that in [9], the resulting 3D visualization mesh is composed of polyhedra instead of tetrahedra.

We devise the method as follows. First, given a 4D unstructured pentatopic mesh and a hyperplane, we compute element-by-element the intersection of the hyperplane with the element edges. We only consider the intersections that lead to a 4D point, and we ignore all the singular intersections leading to either the null set or the full edge. Then, for the current element, we check if the resulting set of selected points generates a 3D polyhedron. If the points in the hyperplane define a volume, we compute the coordinates of the 4D points expressed in terms of a 3D orthonormal base of the hyperplane. Then, we compute a Delaunay tetrahedralization of the resulting 3D points. Finally, we store a link between the intersection edge points and a unique edge identifier. If the intersection points do not define a volume, we continue with the following element. Using the link between the intersection edge points and the unique edge identifiers, we can now merge all the local Delaunay tetrahedralizations to obtain a 3D conformal unstructured tetrahedral mesh, without duplicates of the edge points, that represents the 3D slice of the 4D mesh.

II. Results

We consider the gravitational potential of two masses, defined by Equation (1), such that the positions of the masses evolve in time.

$$V(\vec{x},t) = -G\left(\frac{m_1}{\|\vec{x}-\vec{p}_1(t)\|} + \frac{m_2}{\|\vec{x}-\vec{p}_2(t)\|}\right) \qquad (1)$$

Initially, at time $t = 0$ the two masses are located at different points of the z-axis. Then, the masses will move along the z-axis with constant velocity and opposite direction until they arrive at the same position at $t = 1$, see Equation (2).

$$\begin{aligned} \vec{p}_1(t) &= \vec{p}_1 + (0,0,vt),\ \vec{p}_1 \in \mathbb{R}^3 \\ \vec{p}_2(t) &= \vec{p}_2 - (0,0,vt),\ \vec{p}_2 \in \mathbb{R}^3 \end{aligned} \qquad (2)$$

Hence, the isosurface of the gravitational potential will evolve from two connected components merging into a single component. For a fixed isovalue the gravitational potential defines an implicit 3D manifold embedded into a 4D space (3D space + 1D time). We adapt a 4D pentatopic mesh [7] of a hypercube to capture the 3D embedded manifold defined by the isovalue $V(\vec{x},t) \approx -10$. Then, we obtain a 4D pentatopic mesh composed of 16798112 pentatopes and 879778 nodes. To select the elements to refine first, we compute the elements that intersect the manifold. Then, from those elements, we compute the manifold curvature of each one using the Hessian of $V(\vec{x},t)$ and we select to refine the 10% of the elements with higher curvature. Therefore, the obtained mesh will be refined close to the isosurface and, in particular, where the curvature is higher. The elements near to the isosurface will be smaller than the far one, which will be coarser.

Figure 1 shows three slices at different times. Each time slice is represented using a 3D mesh in the (z,x,y) space. The figures on the left, Figures 1(a), 1(c) and 1(e), illustrate the adapted mesh at times $t = 0$, $t = 0.5$ and $t = 1$ respectively. In the right hand side, Figures 1(b), 1(d) and 1(f), illustrate the adapted mesh with the associated isosurface at times $t = 0$, $t = 0.5$ and $t = 1$ respectively. As we expected, the mesh is more refined close to the isosurface and is coarser far from it. We are showing three different slices in time, but since the presented visualization is a post-process algorithm and we are working with a single 4D pentatopic mesh, we can make as many slices as we require. Figure 2 illustrates a slice with the hyperplane $x = 0.5$. We obtain a 3D space-time configuration in which vertical axis is the time axis. We can see the two initial connected components at the bottom of the mesh, and how they merge to a single connected component.

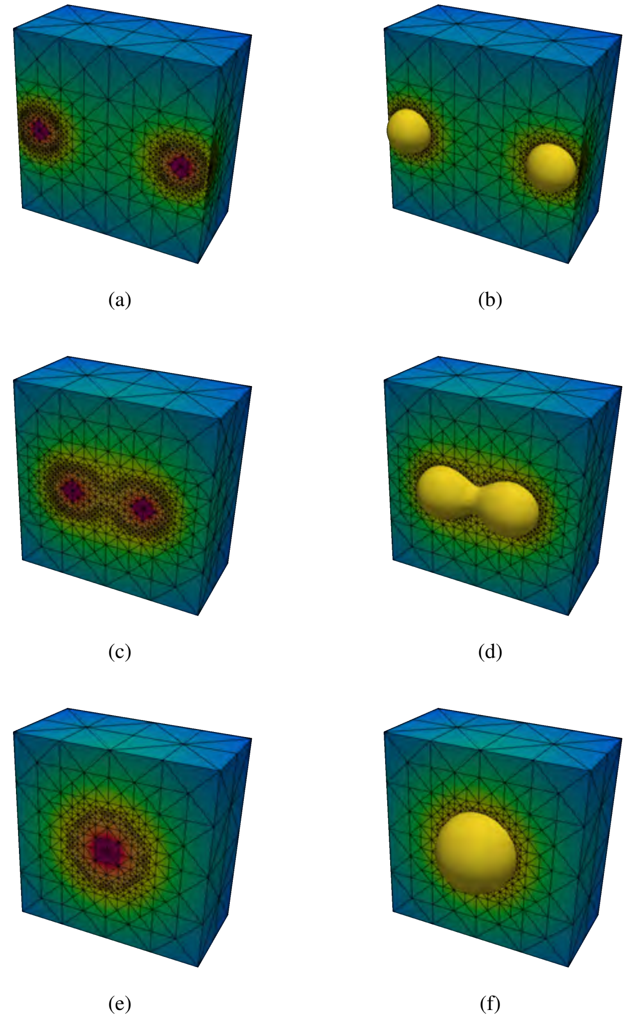

Fig. 1. Different slices in time of an adapted 4D pentatopic mesh are presented. Figures (a) and (b) corresponds to the time slice $t = 0.0$. Figures (c) and (d) corresponds to the time slice $t = 0.5$. Finally, Figures (e) and (f) corresponds to the time slice $t = 1.0$.

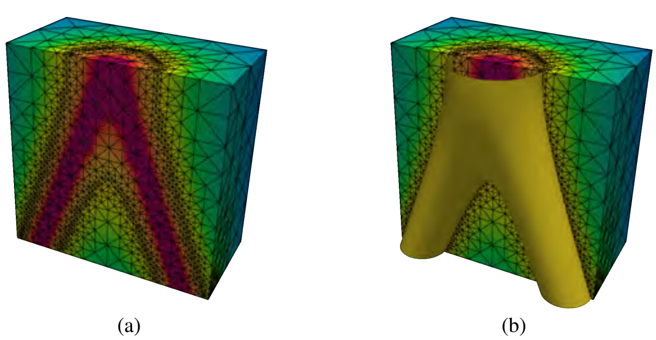

Fig. 2. A slice of an adapted 4D pentatopic mesh with the hyperplane $x = 0.5$ is presented. We obtain the 3D space-time mesh (z, y, t), where we can see the time evolution of the isosurface defined by the gravitational potential.

III. Conclusions

Our preliminary results show that our approach is suitable to visually explore 4D unstructured meshes with the help of 3D visualization interactive packages This capability has facilitated developing, debugging, and checking our 4D bisection method, and thus, we think it might be useful when devising new 4D meshing methods. Furthermore, it allows visualizing 4D scalar fields, which is a crucial feature for our space-time applications.

IV. Acknowledgment

This project has received funding from the European Research Council (ERC) under the European Union's Horizon 2020 research and innovation programme under grant agreement No 715546. This work has also received funding from the Generalitat de Catalunya under grant number 2017 SGR 1731. The work of X. Roca has been partially supported by the Spanish Ministerio de Economía y Competitividad under the personal grant agreement RYC-2015-01633. We would like to thank Dr. Abel Gargallo-Peiró for the fruitful conversations and comments.

References

[1] P. Foteinos and N. Chrisochoides, "4d space-time delaunay meshing for medical images," *Engineering with Computers*, vol. 31, no. 3, pp. 499–511, 2015.

[2] E. Karabelas and M. Neumüller, "Generating admissible space-time meshes for moving domains in $d + 1$-dimensions," *arXiv preprint arXiv:1505.03973*, 2015.

[3] J. M. Maubach, "Local bisection refinement for n-simplicial grids generated by reflection," *SIAM Journal on Scientific Computing*, vol. 16, no. 1, pp. 210–227, 1995.

[4] C. T. Traxler, "An algorithm for adaptive mesh refinement in n dimensions," *Computing*, vol. 59, no. 2, pp. 115–137, 1997.

[5] R. Stevenson, "The completion of locally refined simplicial partitions created by bisection," *Mathematics of computation*, vol. 77, no. 261, pp. 227–241, 2008.

[6] M. Alkämper, F. Gaspoz, and R. Klöfkorn, "A weak compatibility condition for newest vertex bisection in any dimension," *SIAM Journal on Scientific Computing*, vol. 40, no. 6, pp. A3853–A3872, 2018.

[7] G. Belda-Ferrín, A. Gargallo-Peiró, and X. Roca, "Local bisection for conformal refinement of unstructured 4d simplicial meshes," in *International Meshing Roundtable*. Springer, 2018, pp. 229–247.

[8] J. Grande, "Red–green refinement of simplicial meshes in d dimensions," *Mathematics of Computation*, vol. 88, no. 316, pp. 751–782, 2019.

[9] P. C. Caplan, "Four-dimensional anisotropic mesh adaptation for space-time numerical simulations," Ph.D. dissertation, Aero/Astro Dpt., MIT, 2019.

Guillem Belda-Ferrín received his BSc degree in Mathematics from Universitat Politècnica de Catalunya (UPC), Barcelona in 2014. He completed his MSc degree in Advanced Mathematics and Mathematical Engineering from UPC in 2015. Since 2017, he has been with the Geometry and Meshing for simulations group of Barcelona Supercomputing Center (BSC) as a PhD candidate of the Applied Mathematics doctorate program of UPC, Spain.